

This article was downloaded by: [Puzic, Aleksandar]

On: 13 April 2010

Access details: Access Details: [subscription number 921291080]

Publisher Taylor & Francis

Informa Ltd Registered in England and Wales Registered Number: 1072954 Registered office: Mortimer House, 37-41 Mortimer Street, London W1T 3JH, UK



## Synchrotron Radiation News

Publication details, including instructions for authors and subscription information:

<http://www.informaworld.com/smpp/title~content=t716100695>

### Photon Counting System for Time-resolved Experiments in Multibunch Mode

Aleksandar Puzic <sup>a</sup>; Timo Korhonen <sup>a</sup>; Babak Kalantari <sup>a</sup>; Jörg Raabe <sup>a</sup>; Christoph Quitmann <sup>a</sup>; Patrick Jüllig <sup>b</sup>; Lars Bommer <sup>b</sup>; Dagmar Goll <sup>b</sup>; Gisela Schütz <sup>b</sup>; Sebastian Wintz <sup>c</sup>; Thomas Strache <sup>c</sup>; Michael Körner <sup>c</sup>; Daniel Markó <sup>c</sup>; Chris Bunce <sup>c</sup>; Jürgen Fassbender <sup>c</sup>

<sup>a</sup> Paul Scherrer Institut, Villigen, Switzerland <sup>b</sup> Max-Planck-Institut für Metallforschung, Stuttgart, Germany <sup>c</sup> Forschungszentrum Dresden-Rossendorf, Dresden, Germany

Online publication date: 13 April 2010

**To cite this Article** Puzic, Aleksandar , Korhonen, Timo , Kalantari, Babak , Raabe, Jörg , Quitmann, Christoph , Jüllig, Patrick , Bommer, Lars , Goll, Dagmar , Schütz, Gisela , Wintz, Sebastian , Strache, Thomas , Körner, Michael , Markó, Daniel , Bunce, Chris and Fassbender, Jürgen(2010) 'Photon Counting System for Time-resolved Experiments in Multibunch Mode', Synchrotron Radiation News, 23: 2, 26 – 32

**To link to this Article:** DOI: 10.1080/08940881003702056

**URL:** <http://dx.doi.org/10.1080/08940881003702056>

## PLEASE SCROLL DOWN FOR ARTICLE

Full terms and conditions of use: <http://www.informaworld.com/terms-and-conditions-of-access.pdf>

This article may be used for research, teaching and private study purposes. Any substantial or systematic reproduction, re-distribution, re-selling, loan or sub-licensing, systematic supply or distribution in any form to anyone is expressly forbidden.

The publisher does not give any warranty express or implied or make any representation that the contents will be complete or accurate or up to date. The accuracy of any instructions, formulae and drug doses should be independently verified with primary sources. The publisher shall not be liable for any loss, actions, claims, proceedings, demand or costs or damages whatsoever or howsoever caused arising directly or indirectly in connection with or arising out of the use of this material.

# Photon Counting System for Time-resolved Experiments in Multibunch Mode

ALEKSANDAR PUZIC<sup>1</sup>, TIMO KORHONEN<sup>1</sup>, BABAK KALANTARI<sup>1</sup>, JÖRG RAABE<sup>1</sup>, CHRISTOPH QUITMANN<sup>1</sup>, PATRICK JÜLLIG<sup>2</sup>, LARS BOMMER<sup>2</sup>, DAGMAR GOLL<sup>2</sup>, GISELA SCHÜTZ<sup>2</sup>, SEBASTIAN WINTZ<sup>3</sup>, THOMAS STRACHE<sup>3</sup>, MICHAEL KÖRNER<sup>3</sup>, DANIEL MARKÓ<sup>3</sup>, CHRIS BUNCE<sup>3</sup>, AND JÜRGEN FASSBENDER<sup>3</sup>

<sup>1</sup>Paul Scherrer Institut, Villigen, Switzerland

<sup>2</sup>Max-Planck-Institut für Metallforschung, Stuttgart, Germany

<sup>3</sup>Forschungszentrum Dresden-Rossendorf, Dresden, Germany

Pulsed temporal structure of synchrotron radiation (SR) at 3<sup>rd</sup> generation light sources allows for time-resolved studies of dynamic processes with sub-ns ( $\sim 100$  ps) time resolution, given mainly by the temporal width of individual photon flashes. A single flash has low intensity, which inhibits “single-shot” measurements. Therefore, time-resolved experiments have to be performed in a stroboscopic way, accumulating the signal over time periods considerably longer than the duration of the effect of interest. In the commonly used *pump-probe* arrangement, the sample is excited by a *pump* pulse at the time  $t = 0$  and a photon pulse *probes* the sample state after a defined time delay step  $\Delta t$ . This sequence is repeated continuously, integrating the signal until the necessary signal-to-noise ratio (SNR) is reached. The maximum repetition rate of pump pulses depends on the intrinsic relaxation time of the investigated sample. Dynamic response is recorded until the sample reaches equilibrium by increasing the relative time delay of the probing flashes in multiples of  $\Delta t$ . The repetition rate of probing flashes results from the timing parameters and the operation mode of the storage ring. Main timing parameters of the Swiss Light Source (SLS) are summarized in Table 1.

SLS operates in *multibunch* mode with 390 consecutively filled buckets and a gap of 90 buckets. This filling pattern results in  $\approx 500$  MHz repetition rate of photon flashes. The detection of probe pulses and subsequent signal processing have to be sufficiently fast in order to distinguish the two states of the sample separated from one another by

Table 1: Timing parameters of the SLS storage ring

Parameter	Value
Accelerating Frequency (RF)	499.65 MHz
Accelerating Period	$\approx 2$ ns
# buckets (N)	$480 = 32 \cdot 3 \cdot 5$
filled buckets $N_f$	$390 = 6 \cdot 64 + 6$
Revolution Frequency (RF/N)	1.042 MHz
Ring-Revolution-Period	0.9597 $\mu$ s

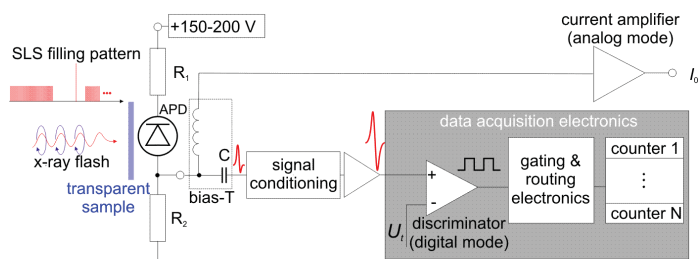


Figure 1: Block scheme of the detection and data acquisition system for time-resolved measurements in multibunch mode. The set-up is based on fast detection of single events and their subsequent digitalization, distribution, and counting.

only  $\approx 2$  ns in time. In general, photon pulses with short duration, low intensity, and high repetition rate pose extreme demands on the detectors and their electronic read-out. Signal-integrating areal detectors, like CCD sensors, have a slow response and cannot be read out fast because of the large number of pixels [1]. For this case, SR sources offer dedicated operation modes for time-resolved measurements, having a low number of bunches with high temporal separation. At the SLS, a single bucket in the gap of the filling pattern is filled for this purpose. The gap width of 180 ns facilitates gating of the detector during the multibunch train while probing the sample with the isolated, high-intensity *camshaft* pulse only [2].

If an experiment allows the use of a fast point detector, a different approach can be employed, which enables the detection and signal processing at 500 MHz data rate. Avalanche photodiodes (APDs) are capable of direct X-ray detection with single photon sensitivity [3]. They exhibit high SNR due to the internal amplification. Off-the-shelf devices with small active area ( $\varnothing \leq 500$   $\mu$ m, [4, 5]) exhibit very fast response with rise time in the range of 100-400 ps. They can easily resolve the time structure of multibunch operation mode. Using this kind of detector in combination with fast read-out

and a dedicated data processing board one is able to continuously distribute the signals originating from the consecutive dynamic states of the sample into distinct channels. The advantage of this approach is that it circumvents the common problem of the repetition rate limitations in a pump-probe scheme, caused by the slow detector read-out and/or long recovery time of the sample. In addition, the experiments can benefit from shorter measurement times, resulting from the use of full photon flux of the multibunch operation mode. Utilizing the flexible concept of programmable hardware [6], various timing configurations can be implemented. A conceptual block scheme of such detection and data acquisition system is shown in Figure 1.

The development of a multichannel data acquisition system is motivated by the demand for time-resolved techniques at several beamlines at the SLS. By taking into account their requirements, we made a collection of general features that should be implemented:

- single and multiple photon detection;
- full mapping of the SLS filling pattern;
- gating of empty buckets and the camshaft; routing of distinct bunches into dedicated counters;

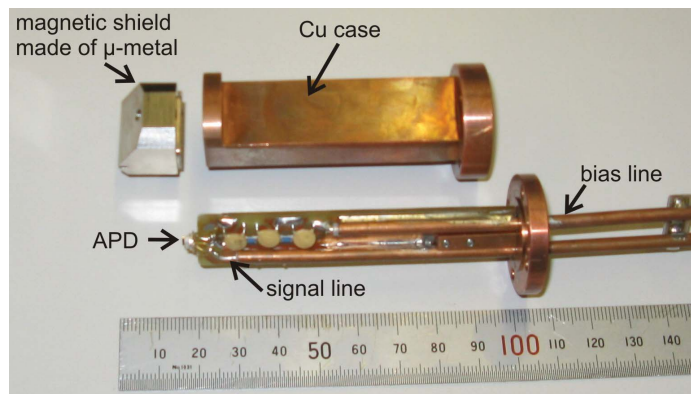


Figure 2: APD-detector used for time-resolved experiments at the SLS-STXM.

- timing reference and trigger signals for diagnostics and synchronization of excitation electronics;
- option for different routing schemes for a certain number of the filling pattern revolutions in the storage ring.

# BRUSHWELLMAN

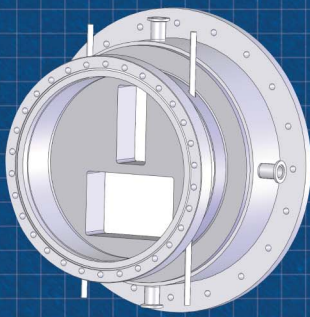
ELECTROFUSION PRODUCTS

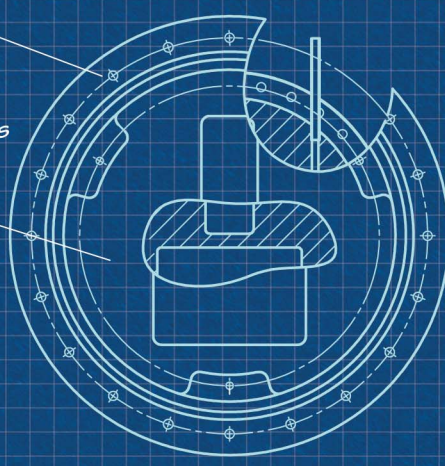
CALL NOW TO DISCUSS YOUR PROJECT  
+1 (510) 623-1500

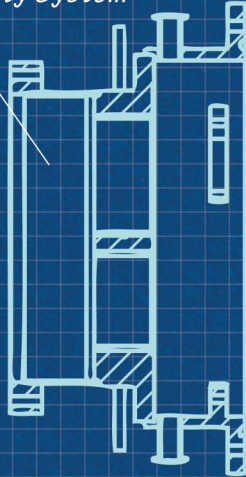
*Actively cooled assemblies, chambers,  
beam pipes and custom engineering*

*Beryllium experts since 1966  
ISO 9001:2008 Quality System*

*Lifetime\* warranty on Be products  
\*Inquire for details*







44036 SOUTH GRIMMER BLVD.  
FREMONT, CALIFORNIA, USA 94538  
WWW.ELECTROFUSIONPRODUCTS.COM  
ELECTROFUSION@BRUSHWELLMAN.COM



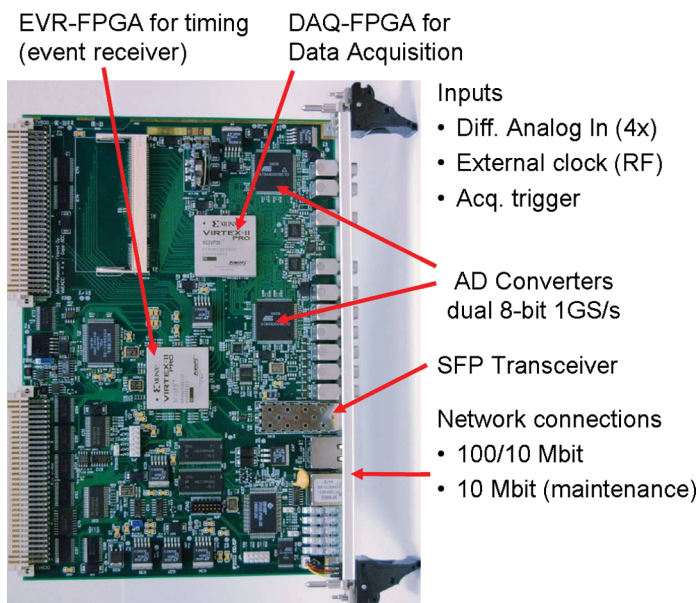


Figure 3: Data acquisition card VME-ADC-200.

Additionally the acquisition system has to be easily reconfigurable and adaptable to different experimental needs due to different relaxation times or different frequency ranges of the investigated samples. In the following we describe a particular realization of this concept for the Scanning Transmission X-ray Microscope (STXM).

### Reconfigurable multichannel counting system at the SLS-STXM

The STXM at the PoLux beamline of the SLS provides nanoscale lateral resolution (15-30 nm) and sub-eV energy resolution in the soft X-ray energy range between 250 and 1200 eV [7]. Circularly polarized radiation from a bending magnet enables magnetic imaging by using X-ray Magnetic Circular Dichroism (XMCD). Equipped with a fast APD-detector and corresponding data acquisition scheme, the STXM can be used for time-resolved imaging of magnetization dynamics [8]. Main components of the APD-detector are outlined in the left part of Figure 1. A photograph of the detector used at the SLS-STXM is given in Figure 2.

For the time-resolved detection of soft X-ray flashes we have selected APDs having a fast time response combined with active areas that match the optical arrangement of the microscope [4, 5]. The average flux at the sample site of the SLS-STXM amounts to approximately one photon per bunch, which makes the implementation of *single photon counting* straightforward. The number of counts in a certain time interval corresponds to the beam intensity transmitted through the sample.

A custom data acquisition card is used for the digitization of APD pulses, as well as for the implementation of the gating, routing, and counting electronics (cf. Figure 3[9]).

This card was initially designed for monitoring of the filling pattern and for the feedback of the top-up injection at the SLS, having features that are an almost perfect match for the present application: two high-speed ADCs (dual-channel, 8-bit, maximum sampling rate of 1 GS/s) with programmable delay enable discrimination between single and multiple photon events, and two fully reconfigurable Virtex-II Pro FPGAs (Field Programmable Gate Arrays) with embedded processors (CPUs), which enable flexible customization of timing, data acquisition, and data processing. Integration into the SLS timing infrastructure is done by the Event Receiver (EVR), implemented in the EVR-FPGA. The EVR recovers the storage ring RF and derives other timing and trigger signals from the global event distribution

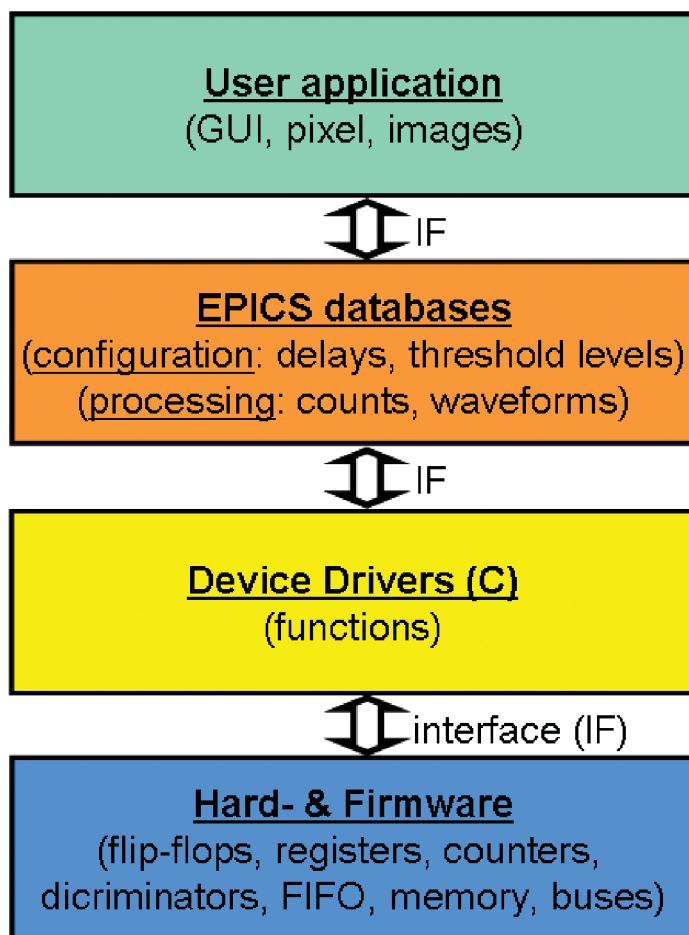


Figure 4: Hard- and software layers of the data acquisition system.

system, like the ring revolution clock ( $RF/480 = 1.042$  MHz), the synchronization for electronic signal generators and pulsers ( $RF/50 \approx 10$  MHz), and the signal for the gating of the top-up injections [10, 11]. The EVR-FPGA provides access to the VME bus, as well as connections to the Ethernet and the RS232 debugging port. The processing of the data sampled by the ADCs is implemented in the DAQ-FPGA. The embedded CPU controls the ADC setting and manages the communication with internal and external busses and ports. The two FPGAs are interconnected via RocketIO links. The firmware programming is done with Xilinx development tools [12]: Integrated Software Environment (ISE) is used for the design entry, implementation, and verification of the functionality. Programming of the embedded processor tasks is done with the Embedded and Software Development Kit (EDK & SDK).

The overall set-up can be structured into one layer of timing and data acquisition hardware and three layers of software (cf. Figure 4). Device drivers, written in C programming language, control the low-level

functions of the hardware. The configuration of the hardware, communication protocols, and additional processing of digital data (counts and waveforms) is done on the next abstraction level using the EPICS toolkit [13]. In the top software layer, the user applications for data acquisition and the control of time-resolved measurement is implemented. The Graphical User Interface (GUI) is programmed using the LabWindows software package.

The overview of the whole set-up for time-resolved imaging at the SLS-STXM is given in Figure 5. The measurement of the electronic pulses coming from the APD detector is done with an ADC operating at 500 MS/s sampling rate, which is sufficient for this particular implementation. The ADC delivers two 8-bit samples every clock period. Double data rate flip-flops (DDR-FF) are used for the first stage of pulse distribution. The samples are subsequently digitally discriminated to 1-bit (1 or 0, depending on the sample value relative to the discrimination threshold). The counters, which are defined in the firmware as 16-bit registers, accumulate these values. In addition,

Downloaded By: [Puzic, Aleksandar] At: 19:49 13 April 2010





# Advanced Undulator !

— Design & Manufacturing —



Courtesy of Spring-8



Courtesy of KEK



## Hitachi Metals, Ltd.

<http://www.hitachi-metals.co.jp/e/index.html>

**Hitachi Metals America, Ltd. Tel +1-224-366-8221**

**Hitachi Metals Europe GmbH Tel +49-7152-939-751**

**NEOMAX ENGINEERING Co., Ltd. Tel +81-3-5765-4250**

**E-mail [neo.horimoto@hitmet.com](mailto:neo.horimoto@hitmet.com)**

**E-mail [tkamiyama@hitachi-metals-europe.com](mailto:tkamiyama@hitachi-metals-europe.com)**

**E-mail [Sachio\\_Hirano@hitachi-metals.co.jp](mailto:Sachio_Hirano@hitachi-metals.co.jp)**



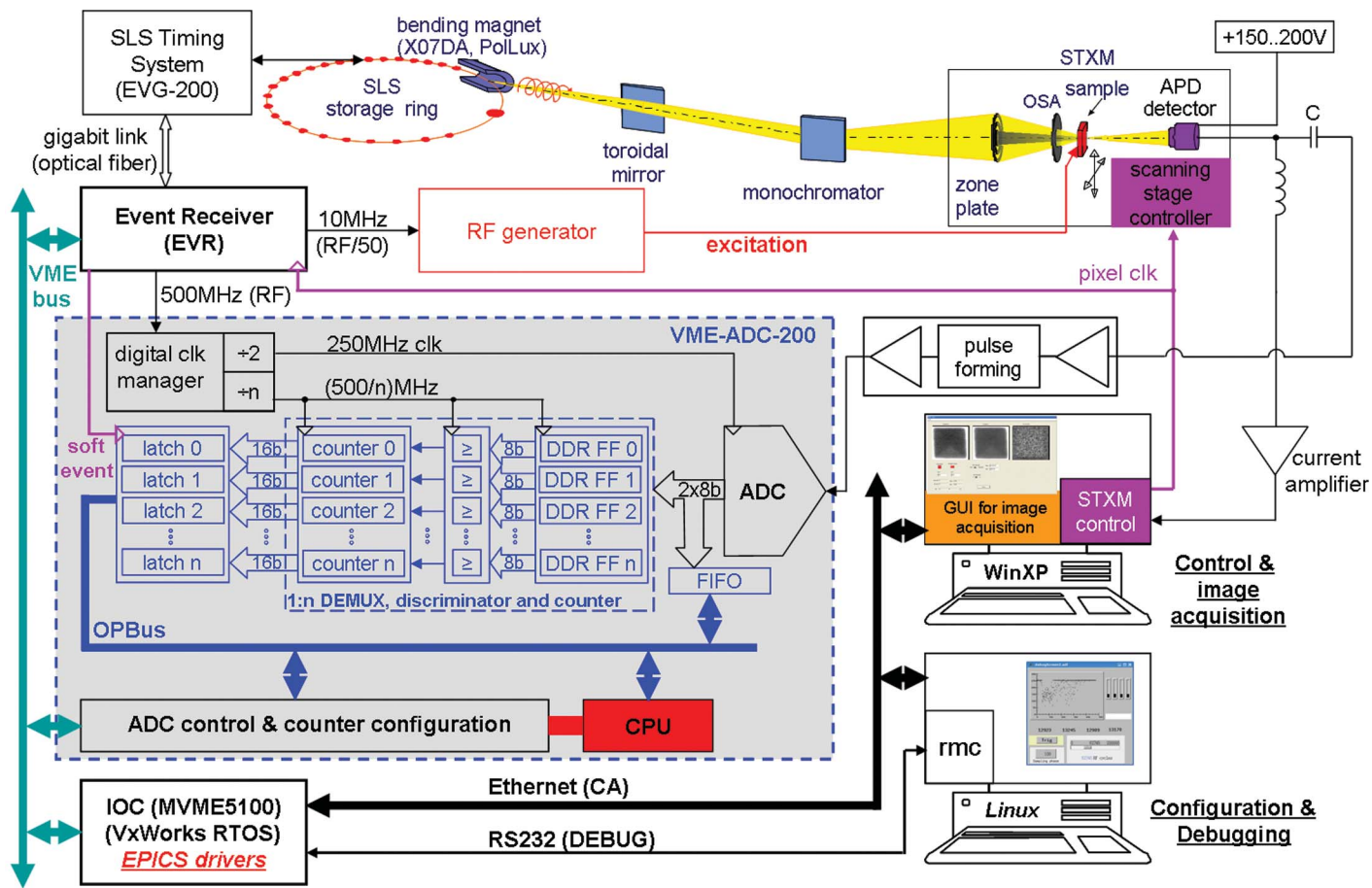


Figure 5: Overview of the whole set-up for time-resolved imaging at the SLS-STXM. Main hardware, firmware, and software components involved in the synchronous multichannel data acquisition system are shown.

the raw ADC samples are transferred to a FIFO to enable tuning of the sampling phase and the setting of the discriminator level (waveform processing).

The distribution, discrimination, and counting of the APD pulses have to occur synchronously with the timing of the storage ring. Therefore, a digital clock manager (DCM) is used in the DAQ-FPGA to regenerate the clock from the RF and to provide all the necessary sub-clocks. The clocking of the digital signal chain is strictly related to the number of counter channels. For experiments in the time domain, the number of channels  $n$  in a pump-probe set-up depends on the relaxation time  $\tau$  of the sample and has to be  $n > \tau / (2 \text{ ns})$ . In the case of measurements in the frequency domain, the number of channels  $n$  is related to the frequency resolution  $\Delta f$  of the setup by the rule  $\Delta f = \text{RF}/n$ .

The signal that starts and stops the counters and the data transfer is the “pixel clock,” which is provided by the STXM scanning

stage controller. This is the only asynchronous signal in the system and has to be “re-sampled” in the EVR-FPGA. Its duration corresponds to the dwell time for a pixel and is equivalent to the total counting time, measured in the number of RF cycles. Typically, accumulation of a single pixel takes 10-100 ms, depending on the transmission of the sample. As a rule of thumb, an image acquisition of a micron-sized area with a resolution of 20 nm ( $\sim (50 \times 50)$  pixel) and “good statistics” takes about 3-10 minutes. When the “pixel clock” changes to “low,” the EVR generates a “soft event,” which initiates the transmission of latched counter values over the OPBus and VME bus into the channels on the Input/Output Controller (IOC) (cf. Figure 5). The IOC is a Motorola VME board that integrates the data acquisition hardware with the EPICS toolkit. A real-time operating system (RTOS) VxWorks runs on the IOC in order to ensure deterministic processing of critical data streams. The deterministic network protocol Channel Access (CA) is used to transfer



the data further to the user application for image acquisition, running on the STXM control PC.

**First results**

The capability of the acquisition system was demonstrated by time-resolved imaging of magnetization dynamics in ferromagnetic microstructures. Magnetic vortex is an ideal system for the initial performance characterization of this set-up since its gyrotropic motion can be excited resonantly on a sub-ns time scale [8]. The images in Figure 6 show snapshots of the magnetization at eight phases of the gyrotropic vortex motion in the cobalt and permalloy layer of the trilayer stack  $Ni_{80}Fe_{20} / Ru / Co$ . The ruthenium interlayer is only 0.825 nm thick and the thickness of each magnetic layer is 25 nm. The sample has lateral dimensions of  $2 \mu m \times 2 \mu m$  and was excited by a sinusoidal magnetic field, alternating at the frequency of 250 MHz. The amplitude of magnetic induction was  $\approx 1.12$  mT. The two vortices move in phase, which can be verified by comparing the contrast patterns of the upper (Co) and lower (Ni) image rows. A synchronous in-phase motion can be


expected in this sample due to the parallel coupling of the magnetization in the two layers.

The capability for measurements in the frequency domain is shown in Figure 7. Resonant response of a square-shaped Co pattern with edge length of  $2 \mu m$  and thickness of 50 nm was investigated as function of the excitation frequency, while using the same excitation amplitude. The sample was excited by an alternating magnetic field  $\mu_0 H = \mu_0 H_0 \sin(2\pi ft)$ , with  $\mu_0 H_0 = 0.8$  mT and  $f = 125$  MHz, 250 MHz and 375 MHz. It can clearly be seen, by the increase of the dynamic effect, that this sample has a resonance peak at  $f = 250$  MHz.

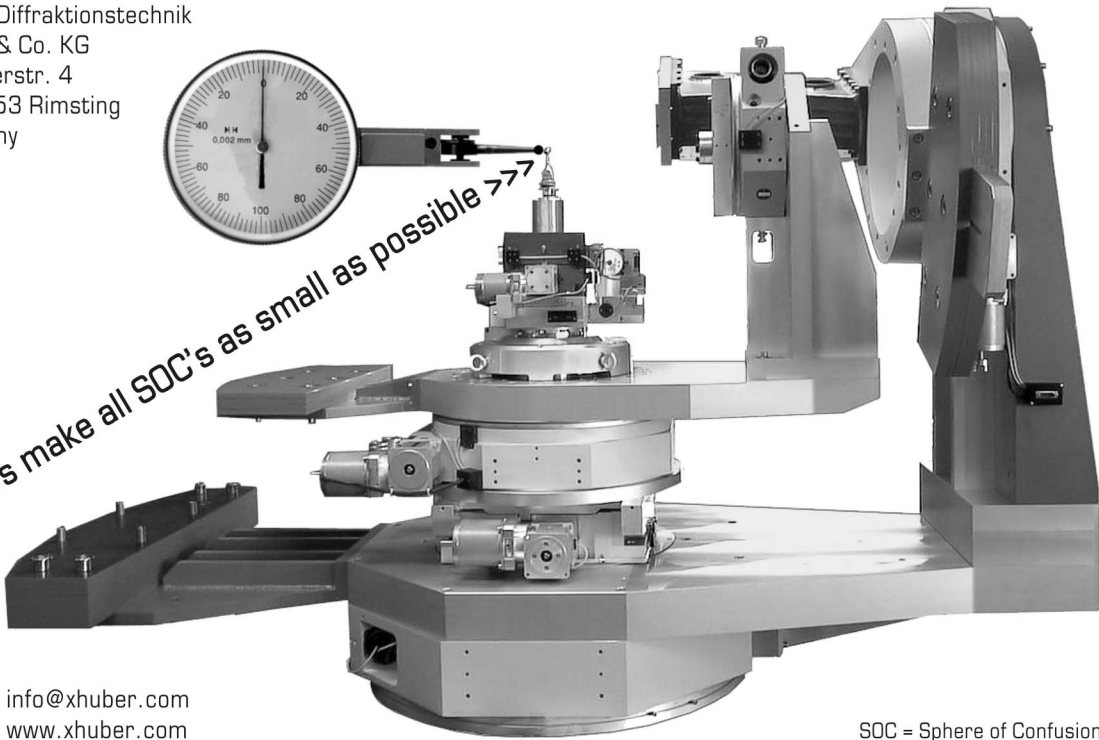
**Conclusion**

The proof of concept and the first implementation of a multi-channel acquisition scheme handling 500 MHz data rate are presented. The functionality and performance were verified by imaging magnetization dynamics in thin-film magnetic microstructures at the SLS-STXM. Initial tests were also performed in the low- $\alpha$  operation

Downloaded By: [Puzic, Aleksandar] At: 19:49 13 April 2010



**HUBER**  
Diffraction and Positioning Equipment



Huber Diffractionstechnik  
GmbH & Co. KG  
Sommerstr. 4  
D-83253 Rimsting  
Germany

Let's make all SOC's as small as possible >>>

info@xhuber.com  
www.xhuber.com

SOC = Sphere of Confusion

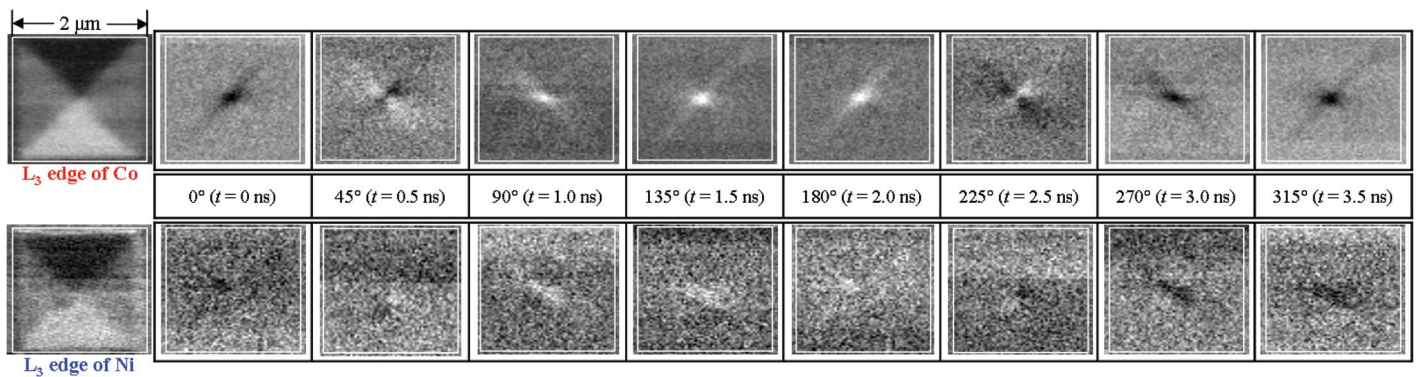


Figure 6: Time- and layer-resolved images of gyrotropic vortex motion in a  $\text{Ni}_{80}\text{Fe}_{20}(25 \text{ nm}) / \text{Ru}(0.825 \text{ nm}) / \text{Co}(25 \text{ nm})$  stack with lateral dimensions of  $(2 \times 2) \mu\text{m}^2$ . The images in the upper and the lower row were acquired with X-ray energies corresponding to the  $L_3$  absorption edges of Co and Ni, respectively. The sample was excited by alternating magnetic induction  $B = B_0 \sin(2\pi ft)$ , with  $B_0 = 1.12 \text{ mT}$  and  $f = 250 \text{ MHz}$ . The images were taken in time steps  $\Delta t = 500 \text{ ps}$  and show the two vortex cores moving mainly in phase.

mode of the SLS (mean electron beam current of 50 mA, temporal width of photon flashes: 5-10 ps). The detection and the data acquisition scheme accommodate lower measurement signals due to the sensitivity and high SNR of the photon counting technique. This creates new possibilities for time-resolved experiments with up to ten times higher temporal resolution, compared to the normal operation mode of the SLS.

Build-up of a similar acquisition system on other beamlines of the SLS is in consideration. However, user friendliness is a big challenge since many details of a particular data acquisition process have to be incorporated. Several levels of different software have to be used to configure and control the complex hardware of the beamline, the end station, and the detector read-out. The firmware programming and the functionality verification of the whole system require substantial effort. Deep understanding of the reconfigurable hardware and mastering of

specialized development tools are necessary for the efficient utilization, debugging and maintenance of the system.

#### Acknowledgements

This work is the result of collaboration between several departments at the Paul Scherrer Institut. We thank Goran Marinkovic for helpful discussions and his assistance in the initial phase of the firmware development. We acknowledge provision of RF equipment by Patrick Pollet from the Diagnostics Group at the SLS. We appreciate the assembly of the APD-detector by Christian Wolter, Sabine Seifert, and Birgit Breimeier at the MPI-MF. The measurements have been performed at the PolLux beamline of the Swiss Light Source, Villigen, Switzerland. The PolLux end station was financed by the German Minister für Bildung und Forschung (BMBF), contract 05 KS4WE1/6.

#### References

1. S. M. Gruner et al., *Rev. Sci. Instrum.* **73**, 2815 (2002).
2. C. Quitmann et al., *Nucl. Instrum. Meth. Phys. Res. A*, **588**, 494, (2008).
3. A. Q. R. Baron et al., *J. Synchrotron Rad.* **13**, 131-142 (2006).
4. Hamamatsu, Si APD, models S2381 and S2382, <http://www.hamamatsu.de>.
5. Silicon Sensor GmbH, models AD230-8 and AD500-8, <http://www.silicon-sensor.com/>.
6. Y. Acremann et al., *Rev. Sci. Instrum.* **78**, 014702 (2007).
7. J. Raabe et al., *Rev. Sci. Instrum.* **79**, 113704 (2008).
8. A. Puzic et al., *J. App. Phys.* **97**, 10E704 (2005).
9. VME-ADC-200, Micro-Research Finland Oy, <http://www.mrf.fi/>.
10. T. Korhonen et al., *Proceedings of ICALEPCS2001*, San Jose, California, <http://www.slac.stanford.edu/econf/C011127/proceedings.html>
11. B. Kalantari et al., *Proceedings of ICALEPCS2003*, Gyeongju, Korea, <http://accelconf.web.cern.ch/accelconf/ica03/>
12. <http://www.xilinx.com/tools/designtools.htm>
13. <http://www.aps.anl.gov/epics/>

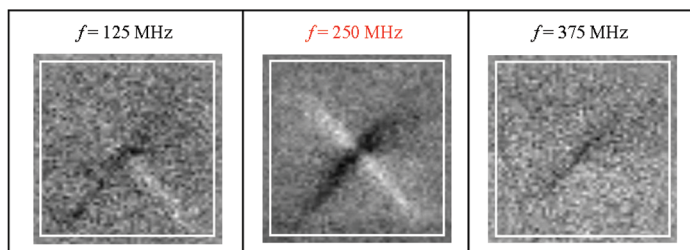


Figure 7: Frequency-resolved imaging of vortex motion in 50-nm-thick, square-shaped Co pattern with edge length of  $2 \mu\text{m}$ . The strongest dynamic response is observed at the frequency  $f = 250 \text{ MHz}$ .